Higher-band gap soliton formation in defocusing photonic lattices

Detlef Kip,[1] Christian E. Rüter,[1] Rong Dong,[1] Zhe Wang,[2] and Jingjun Xu[2]

[1]*Institute of Physics and Physical Technology, Clausthal University of Technology, 38678 Clausthal-Zellerfeld, Germany*

[2]*Key Laboratory of Weak-Light Nonlinear Photonics, Nankai University, Tianjin 300457, China*

Received April 29, 2008; revised August 4, 2008; accepted August 6, 2008;
posted August 13, 2008 (Doc. ID 95536); published September 8, 2008

We report on the experimental observation of higher-band gap solitons in a one-dimensional photonic lattice possessing a defocusing saturable nonlinearity. Pure Floquet–Bloch modes of the first three bands are excited using a prism-coupler setup, and spatial gap solitons of different width are formed, the latter property being related to the increasing anomalous diffraction in the three bands and the fixed value of the nonlinearity in our lithium niobate sample. © 2008 Optical Society of America

OCIS codes: 190.6135, 190.3100, 190.5330.

Light propagation in nonlinear photonic lattices has been intensively studied over the past decade, including both theoretical and experimental investigations [1,2]. An experimental realization of such periodic materials are 1D and 2D arrays of evanescently coupled channel waveguide arrays (WA). On the basis of unique diffraction properties of WA intriguing effects, like discrete normal and anomalous diffraction [3], Bloch oscillations [4,5], as well as light propagation in band structures of multiple allowed bands, separated by gaps, have been explored [6]. When nonlinear material properties are involved, a variety of effects, like discrete modulation instability [7–9] and formation of lattice solitons, has been demonstrated [6,10–12]. Lattice solitons are localized structures that exist owing to the balance of periodicity and nonlinearity. Discrete solitons may be formed in the semi-infinite gap near the top of band one, where beam diffraction is normal, under the influence of a focusing nonlinearity [10]. On the other hand, for gap solitons the propagation constant is shifted inside the gap between two allowed bands. Fundamental gap solitons (inside the first full gap) have been excited either in regions of normal diffraction of lattices with focusing nonlinearity [6,13,14] or from modes of the lowest band experiencing anomalous diffraction, balanced by a defocusing nonlinearity [12,15,16]. For such negative nonlinearities, gap solitons have been observed in honeycomb lattices located in the first final gap between bands 2 and 3 [17]. In other systems, solitons in higher bandgaps have not been investigated, most probably because of difficulties in exciting pure modes of higher bands.

Recently, 1D WAs in $LiNbO_3$ have been fabricated by in-diffusion of Ti, and have served as well-suited optical model systems for investigation of nonlinear wave propagation in periodic media, including soliton formation [12,16]. In this Letter we demonstrate the formation of higher-band discrete solitons having propagation constants inside different finite gaps of a $LiNbO_3$ multiband WA possessing a defocusing photorefractive nonlinearity. For this we apply a new (to the best of our knowledge) method that uses focused light beams coupled into the WA via a high-index prism to excite *pure* Floquet–Bloch (FB) modes in higher bands [18], a problem that can be hardly solved by excitation via the input facet of photonic lattices. Gap solitons of increasing width are formed originating from bands 1, 2, and 3, where this increase is a consequence of increasing anomalous diffraction for higher bands, while the nonlinear index change is fixed.

A 1D WA with period $\Lambda = 10\ \mu m$ is fabricated by Ti in-diffusion using a $LiNbO_3$:Fe wafer. We have determined the band structure of this sample by using a modified mode spectroscopy technique with a prism coupler setup, as described in [18]. The experimental values of the propagation constants and the calculated bandgap diagram, which relates the propagation constant β to the transverse Bloch momentum k_z, are presented in Fig. 1(a). Examples of measured and calculated intensity distributions of FB modes are shown in Fig. 1(b).

The propagation of a coherent light field E along the x direction in a nonlinear WA with periodic index modulation $n = n_{sub} + \Delta n(z)$ is described by the (non-

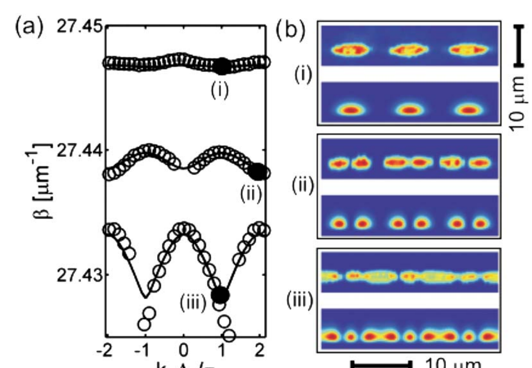

Fig. 1. (Color online) (a) Band structure of the WA. Symbols, experimental values; solid curves, numerical result. (b) Measured (top) and calculated (bottom) intensity profiles of FB modes for (i) band 1 and (iii) band 3 at the edge and (ii) for band 2 in the Brillouin zone center.

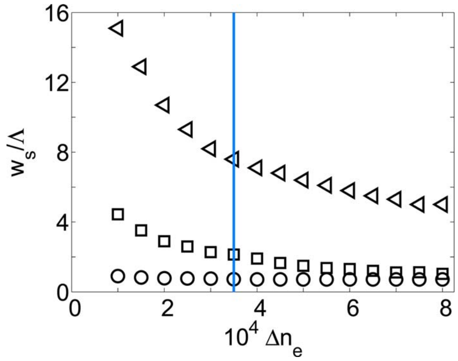

Fig. 2. (Color online) Gap soliton width w_s versus nonlinearity Δn_e. Data are shown for all three bands (bands 1 and 3 for $k_z=\pi/\Lambda$, band 2 for $k_z=0$) and $r=I(z)/I_d=3$. The vertical line shows the experimental situation with fixed value $\Delta n_e=3.5\times10^{-4}$.

linear) paraxial wave equation

$$i\frac{\partial E}{\partial x}+\frac{1}{2k}\frac{\partial^2 E}{\partial z^2}+k(\Delta n(z)+\Delta n_{nl})E=0. \quad (1)$$

Here k is the wave number, n_{sub} is the substrate index, $\Delta n(z)=0.009\cos^2(\pi z/\Lambda)$ is the transverse periodic lattice modulation, and Δn_{nl} is the (saturable) nonlinearity. After solving for the FB modes of the linear system ($\Delta n_{nl}=0$) to obtain the transmission spectrum of Fig. 1(a), we look for soliton solutions of the related nonlinear problem ($\Delta n_{nl}<0$). Gap solitons are found for bands 1 and 3 at Bloch momentum $k_z=\pi/\Lambda$ and for band 2 at $k_z=0$, all in the anomalous diffraction regime.

Next we calculate the FWHM width w_s of gap solitons as a function of nonlinearity using the parameters of our WA. This is done by searching for solitary (self-consistent) solutions in all three guided bands using a nonlinear beam-propagation-method (BPM) code. Then Gaussian profiles are fitted to the obtained intensity profiles (for this we use the maximum of intensity within one lattice period, centered on channel; see inset of Fig. 3) to estimate the FWHM values. In our simulations we have assumed a saturable nonlinearity of the form $\Delta n_{nl}=\Delta n_e r/(1+r)$, where Δn_e is the amplitude of nonlinear refractive index and r is the ratio of light intensity $I(z)$ and dark irradiance I_d. As can be seen in Fig. 2, for fixed

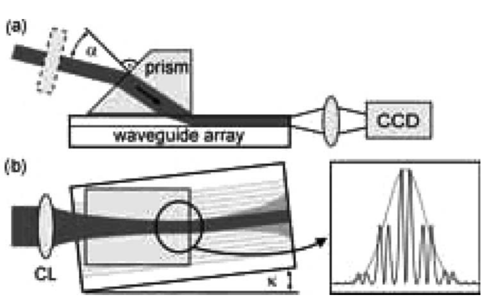

Fig. 3. Scheme of the prism coupler setup used to excite pure FB modes. The cylindrical lens CL focuses the input beam in the z direction only. The inset shows the input Gaussian beam and the corresponding excited FB mode, here for band 2.

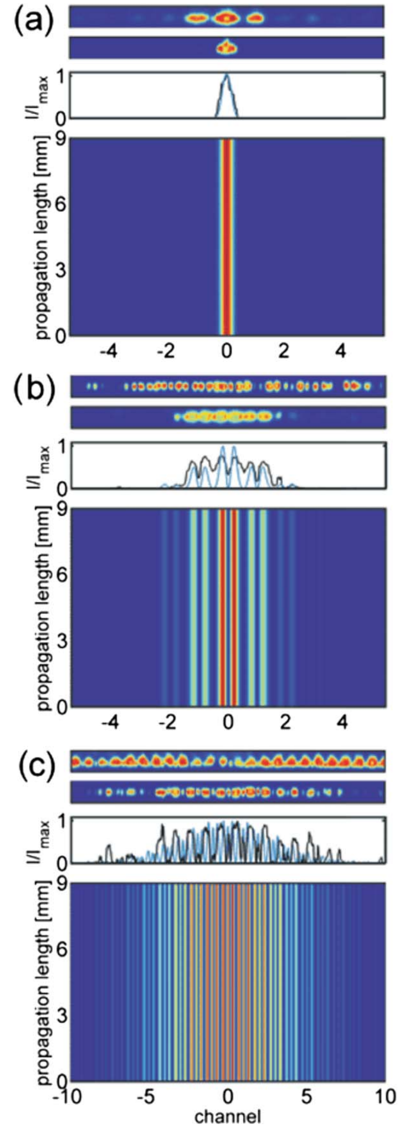

Fig. 4. (Color online) (top rows) Measured linear output intensity profiles, (middle rows) nonlinear case when a soliton is formed, and (lower pictures) nonlinear BPM simulation for bands (a) 1, (b) 2, and (c) 3. The bottom rows, respectively, show experimental (black curve) and BPM line scans (gray curve) of nonlinear output profiles.

nonlinearity Δn_e the soliton width increases for higher bands, which is related to the increasing (anomalous) diffraction coefficient (curvature of bands in Fig. 1). For the investigated range (limited to reasonable values for $LiNbO_3$:Fe) and with increasing nonlinearity, all soliton widths decrease monotonically close to the value $w_{s,th}\sim\Lambda$, i.e. light propagation in a single channel. This behavior is expected, as long as the nonlinear index change is small compared to the width of the respective gap [19].

Experimentally we excite a small number of channels of the WA (i.e., limited spectra of FB modes) by using the prism-coupling method shown schematically in Fig. 3. As has already been mentioned, formation of gap solitons is limited to regions of anomalous diffraction in our defocusing lattice, that is, Bloch momentum $k_z\sim\pi/\Lambda$ for bands 1 and 3 and $k_z\sim0$ for band 2. However, when using the prism coupler, the excitation efficiency of FB modes from higher bands is limited by the overlap of the input plane wave with the respective FB mode amplitude. As a consequence, coupling to band 2 is more effective for Bloch momentum $k_z=2\pi/\Lambda$ (instead of $k_z=0$), and for band 3 we have to choose $k_z=3\pi/\Lambda$ for effective excitation. The input light (wavelength 514.5 nm) is focused in transverse z direction using a cylindrical lens so that the focal point (plane phase front) is located at the coupling region at the prism base. By proper choice of both, the two angles (α, which defines the longitudinal wave vector component β, and tilt angle κ, which defines the Bloch momentum k_z, see [15]) and the input beam diameter impinging on the lens, the excited mode spectra of the WA can be precisely selected (see inset of Fig. 3).

In Fig. 4 the measured output intensity profiles for both, linear propagation (after switching on the light at time $t=0$) and after build-up of the nonlinearity, i.e., when a soliton is formed (after time $t\sim5$ min), are shown. The width of the exciting Gaussian input beam is adjusted to 10, 20, and 80 μm for bands 1, 2, and 3, in accordance with the numerical data from Fig. 2. Results for excitation of bands 1 (a), 2 (b), and 3 (c) are compared with numerical simulations using a BPM. Because of the increasing diffraction for higher bands the corresponding soliton widths increases, and, for the assumed parameters of the nonlinearity, the numerical calculation of these widths (vertical line in Fig. 2) is in fairly good agreement with our experiments.

In conclusion, we have demonstrated spatial discrete solitons in different gaps of a defocusing photonic lattice. Pure FB modes were excited using a modified prism-coupling setup. This newly developed method allows for the investigation of more-complex soliton interactions, for example gap–gap soliton transitions or the formation of optical “excitons,” which are vector solitons having both bright and dark components originating from different bands.

We acknowledge financial support by the Deutsche Forschungsgemeinschaft (KI482/8-2), the German Federal Ministry of Education and Research (CHN 07/040), and the Ministry of Science and Technology of China (2005DFA10170).

References and Notes

1. J. W. Fleischer, G. Bartal, O. Cohen, T. Schwartz, O. Manela, B. Freedman, M. Segev, H. Buljan, and N. K. Efremidis, Opt. Express **13**, 1780 (2005).
2. D. N. Neshev, A. A. Sukhorukov, W. Królikowski, and Yu. S. Kivshar, J. Nonlinear Opt. Phys. Mater. **16**, 1 (2007).
3. H. S. Eisenberg, Y. Silberberg, R. Morandotti, and J. S. Aitchison, Phys. Rev. Lett. **85**, 1863 (2000).
4. R. Morandotti, U. Peschel, J. S. Aitchison, H. Eisenberg, and Y. Silberberg, Phys. Rev. Lett. **83**, 4756 (1999).
5. T. Pertsch, P. Dannberg, W. Elflein, A. Brauer, and F. Lederer, Phys. Rev. Lett. **83**, 4752 (1999).
6. D. Mandelik, H. S. Eisenberg, Y. Silberberg, R. Morandotti, and J. S. Aitchison, Phys. Rev. Lett. **90**, 053902 (2003).
7. J. Meier, G. I. Stegeman, D. N. Christodoulides, Y. Silberberg, R. Morandotti, H. Yang, G. Salamo, M. Sorel, and J. S. Aitchison, Phys. Rev. Lett. **92**, 163902 (2004).
8. M. Stepić, C. Wirth, C. E. Rüter, and D. Kip, Opt. Lett. **31**, 247 (2006);
9. C. E. Rüter, J. Wisniewski, and D. Kip, Opt. Express **15**, 6320 (2007).
10. H. S. Eisenberg, Y. Silberberg, R. Morandotti, A. R. Boyd, and J. S. Aitchison, Phys. Rev. Lett. **81**, 3383 (1998).
11. J. W. Fleischer, M. Segev, N. K. Efremidis, and D. N. Christodoulides, Nature **422**, 147 (2003).
12. F. Chen, M. Stepić, C. E. Rüter, D. Runde, D. Kip, V. Shandarov, O. Manela, and M. Segev, Opt. Express **13**, 4314 (2005).
13. D. Mandelik, R. Morandotti, J. S. Aitchison, and Y. Silberberg, Phys. Rev. Lett. **92**, 093904 (2004).
14. D. Neshev, A. A. Sukhorukov, B. Hanna, W. Królikowski, and Yu. S. Kivshar, Phys. Rev. Lett. **93**, 083905 (2004).
15. J. W. Fleischer, T. Carmon, M. Segev, N. K. Efremidis, and D. N. Christodoulides, Phys. Rev. Lett. **90**, 023902 (2003).
16. M. Matuszewski, C. R. Rosberg, D. N. Neshev, A. A. Sukhorukov, A. Mitchell, M. Trippenbach, M. W. Austin, W. Królikowski, and Yu. S. Kivshar, Opt. Express **14**, 254 (2006).
17. O. Peleg, G. Bartal, B. Freedman, O. Manela, M. Segev, and D. N. Christodoulides, Phys. Rev. Lett. **98**, 103901 (2007).
18. C. E. Rüter, J. Wisniewski, and D. Kip, Opt. Lett. **31**, 2768 (2006).
19. The spatial frequency spectrum of a gap soliton (and the minimum possible width of the soliton) is limited by the size of the respective gap. However, because in our case all gaps (measured in units of effective index) are large compared with the nonlinearity, minimum soliton width is still limited by the maximum nonlinearity of our $LiNbO_3$:Fe sample ($\sim4\times10^{-4}$).